



IMPORTANCE OF SOIL-BRIDGE INTERACTION MODELING IN SEISMIC ANALYSIS OF SEISMIC-ISOLATED BRIDGES

Murat DICLELI¹, Jung -Yoon LEE² and Mohamad MANSOUR³

SUMMARY

The effect of soil-structure interaction on the seismic performance of seismic-isolated bridges is studied. For this purpose, two typical seismically isolated bridges are selected. The selected bridges have distinct features to represent those bridges with (i) heavy superstructure and light substructure and (ii) light superstructure and heavy substructure. Detailed structural models of both bridges excluding and including the soil-structure interaction effects are first constructed. Iterative multi-mode response spectrum analyses of the bridges are then conducted considering the nonlinear behavior of the isolation bearings. The analyses results have revealed that soil-structure interaction effects may be neglected in the seismic analysis of seismic-isolated bridges with heavy superstructure and light substructure constructed on stiff soil. However, the soil-structure interaction effects need to be considered for bridges with light superstructure and heavy substructures regardless of the stiffness of the foundation soil. In soft soil conditions, soil structure interaction effects need to be considered regardless of the bridge type.

INTRODUCTION

The soil-structure interaction (SSI) effects and the contribution of the higher modes of vibration are commonly ignored in the earthquake resistant design of seismically isolated bridges. These simplifications are done assuming that the flexibility of the isolation system and the isolated modes of vibration dominate the seismic behavior of the bridge. Only limited research has been conducted to study the effect of SSI on the performance of seismic-isolated bridges, Chaudhary [1], Vlassis [2] and buildings, Todorovska [3], Dasgupta [4]. Therefore, further research is required in this area to guide the design engineers to built more accurate structural models of seismic-isolated bridges that may lead to more improved prediction of their seismic response. Accordingly, the objective of this study is to assess the impact of such simplifications on the seismic performance of seismic-isolated bridges.

¹ Asst. Prof., Dept. of Civil Engrg and Construction, Bradley Univ., Peoria, Illinois 61625, USA
E-mail: mdicleli@bradley.com, Tel.: (309) 677-3671, Fax.: (309) 677-2867

² Asst. Prof., Dept. of Architectural Engineering, Sungkyunkwan University, South Korea

³ Resch. Asst. Prof., Dept. of Civil Engineering, University of Houston, Texas, Houston, USA.

In application to bridges, seismic isolation bearings are installed between the substructure and the superstructure. The elevation view of a typical seismically isolated bridge is shown in Fig.1. For the purpose of demonstrating the effect of including the SSI in the seismic analysis, the bridge may simply be idealized as shown in Fig. 1. Note that the rotational stiffness of the soil-foundation system is excluded from the idealized model for the purpose of simplicity. The equivalent fundamental period of such an idealized system is expressed as;

$$T_e = 2\pi \sqrt{m_p \left(\frac{1}{k_s} + \frac{1}{k_p} \right) + m_s \left(\frac{1}{k_s} + \frac{1}{k_p} + \frac{1}{k_i} \right)} \quad (1)$$

where, m_p and m_s are the masses of the sub and superstructure and k_s , k_p and k_i are respectively the equivalent linear stiffness (ELS) of the soil-foundation system, substructure and the seismic-isolation system. The above equation clearly indicates that the equivalent fundamental period, hence the magnitude of the seismic forces acting on a seismic-isolated bridge may be affected by the stiffness of the soil-foundation system, substructure, seismic-isolation system as well as the mass of the sub and superstructure of the bridge.

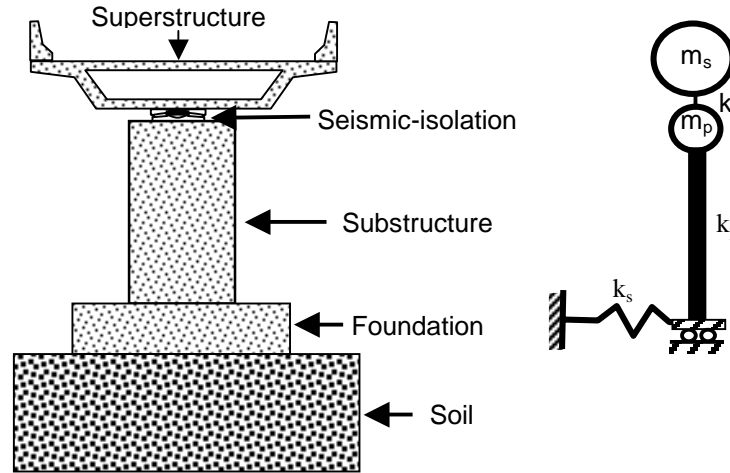


Fig. 1 Typical seismic-isolated bridge and simplified model

Two seismic-isolated bridges with distinct features are selected to investigate the effect of the above-mentioned parameters on the seismic response of seismic-isolated bridges. The first one represents those bridges with heavy superstructure (large m_s) and light substructure (small m_p) and the second one represent those with light superstructure (small m_s) and heavy substructure (large m_p). These features become important in assessing the effect of SSI on the seismic response of seismic-isolated bridges as observed from Eq. 1. Detailed structural models of both bridges excluding and including the SSI effects are first constructed. The bridges are then analyzed using an iterative multi-mode response spectrum (MMRS) analysis technique taking into account the non-linear behavior of the seismic-isolation system and SSI effects. The analyses are performed for stiff and soft foundation soil conditions. Next, the obtained seismic demands with and without the SSI effects are compared to assess the effect of SSI on the seismic response of seismic-isolated bridges.

DESCRIPTION OF THE BRIDGES

The selected bridges are located in the state of Illinois. Their seismic-isolation design was performed as part of a seismic retrofitting study using friction pendulum bearings (FPB). The description of the bridges and the seismic-isolation bearings are outlined in the following subsections.

Bridge I

The first bridge is located in Johnson County, Illinois and represents those bridges with heavy superstructure and light substructure. The bridge has 3 spans carrying two traffic lanes and a slab-on-prestressed-concrete-girder deck as shown in Fig 2. The bridge deck is continuous from one abutment to the other and is supported by two multi-column piers in between. Six FPB are placed at each substructure location.

The abutments are seat type as illustrated in Fig. 2. The abutment and the wingwalls are directly supported on nine HP200X54 steel end-bearing piles, seven of which are placed underneath the abutment. The average length of the end-bearing piles is 4.2 m at the north and 6.2 m at the south abutments. Three of the abutment piles are battered with a slope of 1:6. The piers of the bridge are reinforced concrete multi-column bents and are supported on spread footings resting on stiff soil. The geometric details of the piers are presented in Fig. 2.

The site soil is composed of layers of stiff silty clay extending down to the hard sandstone. The base of the north abutment is placed approximately at the natural ground level while the south abutment is placed approximately 1.7 m above the natural ground level. The fill material above the ground level is medium moist silty clay.

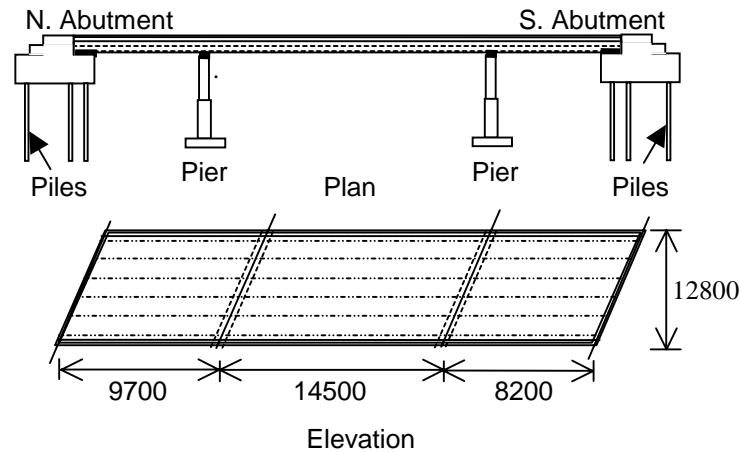


Fig. 2 Bridge-I geometric details

Bridge II

The second bridge is located in Jackson County, Illinois and represents those bridges with light superstructure and heavy substructure. It has three continuous spans carrying two traffic lanes and is supported by two heavy wall-piers as shown in Fig. 3. The bridge superstructure is slab-on-steel-girder. Six FPB are placed at each substructure location. The FPB at the abutments are fixed in the longitudinal direction to prevent the tilting of the abutments under the effect of dynamic active backfill pressure and large seismic inertial forces generated due to the heavy mass of the abutments.

The bridge abutments are seat type as illustrated in Fig. 3. Each abutment is supported on a single row of six 356-mm diameter, #7 gauge metal shell floating piles filled with cast-in-place concrete. Two of the piles are battered at a slope of 1:6. All the piles are embedded 305-mm into the abutments. The average length of the piles is 19 m. The piers are reinforced concrete walls as shown in Fig. 3. Both piers have identical geometry and are supported by three rows of eleven untreated southern pine timber floating piles embedded 152-mm into the pile-cap and driven 8.5-m into the soil. The piles are tapered with a top and bottom end diameters of respectively 305 and 203 mm.

The site soil consists of three distinct layers of clay. The first layer is stiff silty clay extending approximately 9.8 - 16.8 m below the ground surface followed by 4 - 10 m thick layer of stiff moist brown clay. The last layer is hard gray clay shale.

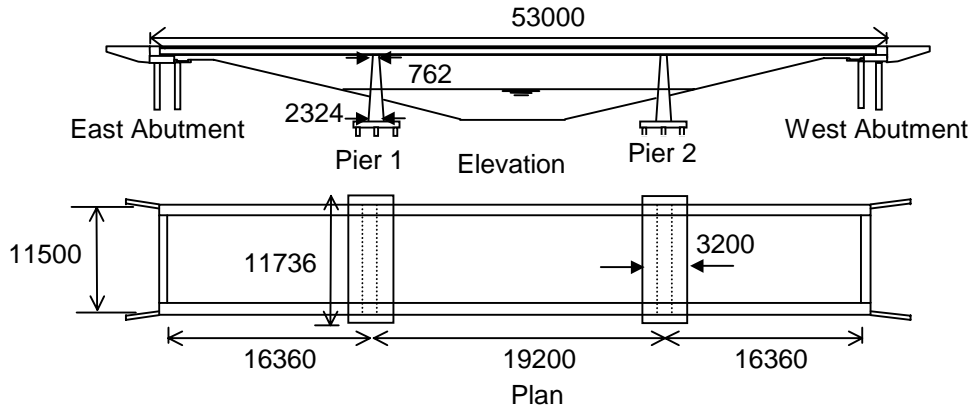


Fig. 3 Bridge-II geometric details

Isolation Bearings

FPB were used for the seismic-isolation design of the bridges. The main components of the bearing, its sliding motion and idealized hysteretic behavior are illustrated in Fig. 4. The envelope of the bearing's hysteresis loop, the ELS, k_i , and equivalent viscous damping ratio (EVDR), ζ_e , of the bearing are defined by the following equations, Dicleli [5]:

$$F = \mu W + \frac{W}{R} D \quad (2)$$

$$k_i = \frac{\mu W}{D_d} + \frac{W}{R} \quad (3)$$

$$\zeta_e = \frac{2}{\pi} \left(\frac{\mu}{\mu + \frac{D_d}{R}} \right) \quad (4)$$

where μ is the friction coefficient at the slider-concave plate interface, W is the weight acting on the bearing, R is the radius of the concave surface and D is the bearing displacement. For the bridges considered in this study, $\mu=4\%$, and $R=1.020$ m. A response spectrum obtained for a viscous damping equal to that produced by the bearings is then used in the analyses to account for the hysteretic energy dissipated by the bearings.

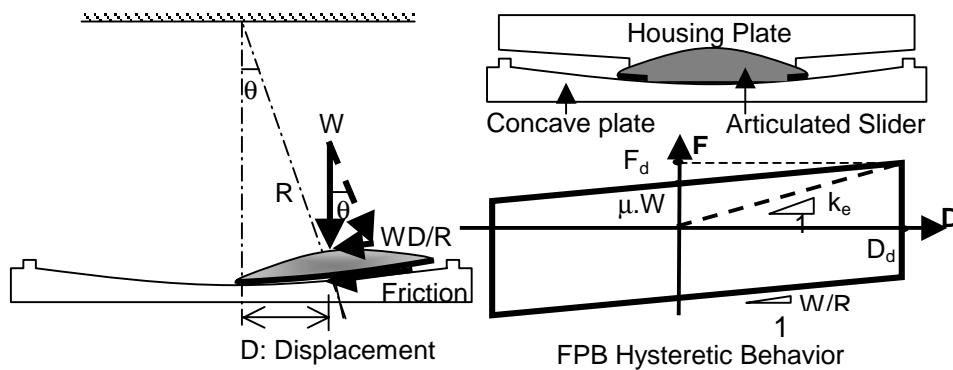


Fig. 4 Characteristics of FPB

TYPES OF SEISMIC ANALYSES

Two sets of seismic analyses of the bridges are conducted using two separate structural models that exclude and incorporate SSI effects for the stiff soil conditions of the bridge sites (referred to as AASHTO [6] (American Association of State Highway Transportation Officials) soil type II throughout the text). Furthermore, the same analyses are repeated assuming fictitious soft soil conditions for the bridge sites to study the effect of the foundation soil stiffness on the performance of seismic-isolated bridges. Two different soft soil conditions are considered in the seismic analyses. In the first case, the stiffness of the fictitious soft soil is assumed to be half the stiffness of the actual stiff soil of the bridge site (referred to as AASHTO soil type III-a throughout the text). In the second case, the stiffness of the fictitious soft soil is assumed to be quarter the stiffness of the actual stiff soil of the bridge site (referred to as AASHTO soil type III-b throughout the text).

In this study, MMRS analysis method is used as recommended by AASHTO [7] Guide Specifications for Seismic Isolation Design for the types of bridges under consideration. Furthermore, AASHTO design spectra are representative of many design earthquake time history records that may be used in the design of bridges. Therefore, the conclusions drawn from a MMRS analysis based on AASHTO design spectra are considered more general compared to using time history analyses based on specific ground acceleration time histories. Accordingly, an iterative MMRS analysis method is used to simulate the non-linear behavior of the FPB and lateral soil-pile interaction effects as will be described later in the subsequent sections of the paper. The normalized acceleration response spectra of AASHTO for soil types II and III are used in the analyses respectively for the stiff and fictitious soft soil conditions. For Bridge I and II, the zonal acceleration ratios are respectively obtained as 0.12 and 0.14 for the bridge sites and used for scaling the normalized acceleration design spectra.

BRIDGE STRUCTURAL MODELS

Structural models of the bridges are built and analyzed using the program SAP2000 [8]. The structural models for Bridge-I including and excluding SSI effects are illustrated in Fig. 5. Those for Bridge-II are similar. These structural models are capable of simulating the nonlinear behavior of the isolation system and SSI effects when used in combination with iterative MMRS analyses.

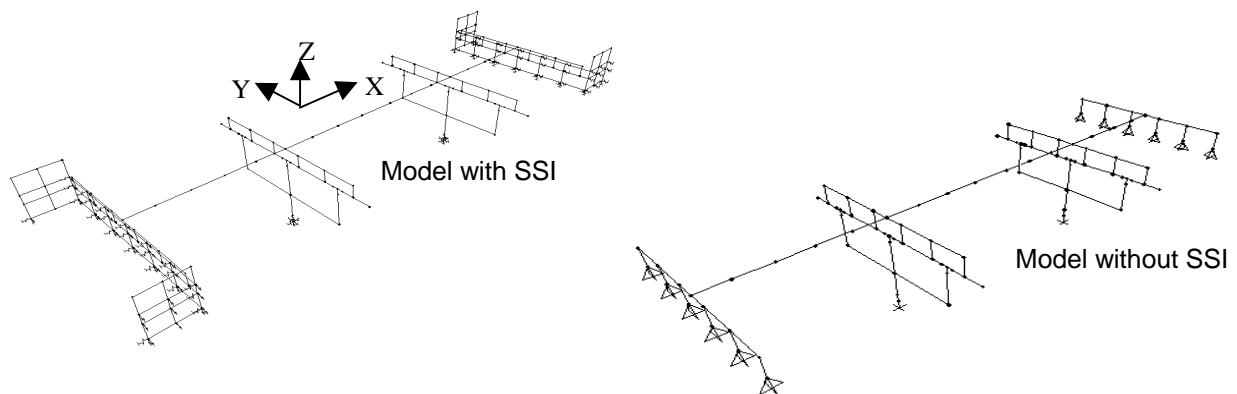


Fig. 5 Structural models of Bridge-I including and excluding SSI effects

SUPERSTRUCTURE MODELING

The superstructures of both bridges are modeled using 3-D beam elements. Full composite action between the slab and the girders is assumed in the models. The superstructures are divided into a number

of segments and their mass are lumped at each nodal point connecting the segments. The large in-plane translational stiffness of the bridge decks is modeled as transverse rigid bars of length equal to the bridge width and connected to the superstructure at the abutments and piers. These rigid bars are used for simulating the interaction between the movements of the bridge superstructure, bearings and substructures.

Isolation Bearings Modeling

The isolation bearings are idealized as 3-D beam elements connected between the superstructure and substructures at girder locations. Pin connection is assumed at the joints linking the bearings to the substructures. The ELS of the bearings as given by Eq. 3 is used in combination with iterative MMRS analyses to simulate their nonlinear behavior.

Substructures Modeling

The pier elements for both bridges are modeled using 3-D beam elements. For Bridge-II, assuming that the wall cross-section remains plane after deformation, the width of the wall is modeled using a horizontal rigid bar connected to the wall top. This enabled the connection of the bearing elements to the wall. The footings of both bridges are also modeled as vertical rigid beam elements to accurately estimate the effect of seismic forces transferred to soil or piles. For the structural model without the SSI effects, the base of the piers is fixed. For the model including the SSI effects, six boundary springs are attached at the base of the piers to model soil-foundation interaction.

The abutments are generally ignored in the structural models of bridges without the SSI effects. Thus, rigid support conditions are assumed at the abutment location as shown in Fig. 5. For the structural model with the SSI effects, the abutments are modeled using a grid of 3-D beam elements as illustrated in Fig. 5. The SSI effects are implemented in the model using boundary springs attached at the interface nodes between the abutment, backfill and the piles as shown in Fig 5.

MODELING PILE-SOIL INTERACTION

At the abutments of both bridges, a vertical and two lateral translational boundary springs are connected to the base of the abutments at each pile location to model the flexibility of the piles. At the piers of Bridge-II, considering the piles' group effect, three translational and three rotational boundary springs are connected to the base of the piers to model the flexibility of the whole foundation system.

Modeling Nonlinear Lateral Pile-Soil Interaction Effects

A two-step procedure is adopted to include the nonlinear lateral pile-soil interaction effects in the seismic analyses of the bridges. In the first step, the pile foundations without the bridge are modeled and nonlinear static pushover analyses are conducted to determine their lateral force-displacement relationships. In the second step, using these nonlinear relationships and an iterative MMRS analysis procedure, ELS's are formulated for the lateral translational springs representing the lateral stiffness of the piles to incorporate the nonlinear lateral behavior of the piles in the analysis.

The ELS is defined as the slope of the secant line connecting the origin to the point representing pile's seismic lateral force on the lateral force-displacement curve of the piles and is obtained following an iterative MMRS analysis procedure as described elsewhere, Dicleli [5]. The ELS of Bridge I and II piles in the global X and Y directions of the bridge are presented in Table 1.

Table 1 Stiffness of boundary springs at foundations

Bridge	Substr.	Pile Type	K_x kN/m	K_y kN/m	K_z kN/m	$K_{\theta x}$ kN.m/rad	$K_{\theta y}$ kN.m/rad	$K_{\theta z}$ kN.m/rad
I	N. Abutment	Vertical	2750	2500	324762	0	0	0
		Battered	25725	2500	315915	0	0	0
	S. Abutment	Vertical	3600	2700	220000	0	0	0
		Battered	12375	2700	214000	0	0	0
	Pier 1	No pile	8620000	10280000	10040000	292000000	40400000	729000000
	Pier 2	No pile	4600000	5.520000	5360000	156000000	21600000	532000000
II	Abutments	Vertical	11810	11810	242861	0	0	0
		Battered	23298	11810	236297	0	0	0
	Piers	Group	78817	55888	1269075	14440604	1257156	832100

Modeling Vertical Pile-Soil Interaction Effects

For the steel H-piles of Bridge-I bearing on hard sandstone, their vertical stiffness is assumed to be independent of the soil properties and equal to their axial stiffness. For the floating piles of Bridge-II, Novak's [9] procedure is used to obtain the vertical stiffness of the piles. The vertical stiffness (stiffness in global Z-direction) of Bridge-I and II piles are presented in Table 1.

Modeling Rotational and Torsional Stiffness of The Pile Group

The stiffness of the rotational springs for the rocking and torsional motion of Bridge-II pier footings is calculated by introducing a unit rotation about the global X, Y and Z axes at the geometric center of the pile group and calculating the moment of the generated elastic pile forces about the geometric center of the pile group. Detailed information about the calculation of stiffness is presented elsewhere, Dicleli [5]. The rotational stiffnesses of the pile group at the piers of Bridge-II are presented in Table 1.

MODELING SPREAD FOOTINGS-SOIL INTERACTION

The soil-footing interaction effect at the piers of Bridge-I is included in the model using three translational and three rotational uncoupled boundary springs connected at the interface nodes of soil and rectangular spread footings. The method proposed by Dobry [10] is employed in the calculation of the stiffness of the boundary springs for the vertical, horizontal, rocking, and torsional modes using the equivalent shear modulus, G and the Poisson ratio of the foundation soil. The equivalent shear modulus is obtained by reducing the initial shear modulus, G_{max} of the foundation soil using a reduction factor of 0.8 considering the seismicity of the site, FHWA [11]. This is done to incorporate the effect of cyclic loading on the properties of the foundation soil. Furthermore, a Poisson ratio of 0.45 is used for the site soil [FHWA, 1997]. The stiffness of the boundary springs are also modified to account for the effect of the embedment depth of the footing following the procedure recommended by FHWA [1997]. More detailed information about the modeling procedure is presented elsewhere [Dicleli and Mansour, 2002]. The results are presented in Table 1.

MODELING BACKFILL-ABUTMENT INTERACTION

Longitudinal Direction

In the longitudinal direction, a series of translational springs are attached to the nodes of only one of the abutments to model the passive resistance of the backfill as shown in Fig. 5. No springs are attached to the other abutment since under seismic loading in the longitudinal direction only one abutment is pushed towards the backfill while the other is pulled away. Thus, two separate structural models are built with springs attached to the left abutment only and to the right abutment only to obtain the seismic response of the bridge. Using the relationship for the variation of the earth pressure coefficient as a function of the

abutment movement defined by Clough [12], the horizontal subgrade constant, k_{sh} , for the backfill is obtained as a function of the depth from the abutment top. The stiffness of the boundary springs at the abutment-backfill interface nodes are then calculated by multiplying k_{sh} by the area tributary to the node.

Transverse Direction

Translational springs are attached to the nodes of only one of the wingwalls at each abutment to simulate the effect of the backfill's passive resistance in the transverse direction since the other wingwall is displaced away from the backfill under the effect of seismic forces. The stiffness of these springs is again calculated by multiplying, k_{sh} by the area tributary to the node on the wingwall. The effect of embankment soil is conservatively neglected in the model.

Translational springs are also attached at each node of the abutment to model the shear stiffness of the backfill. The shear stiffness of the backfill is calculated assuming that only the portion of the backfill between the wing-walls will deform in a shearing mode as the bridge moves in the transverse direction. The stiffness of the transverse boundary springs at the abutment is then obtained by equally distributing the calculated shear stiffness to the interface nodes.

ITERATIVE MMRS ANALYSIS PROCEDURE

An iterative MMRS analysis technique is used to incorporate the nonlinear behavior of the isolation bearings. In the iterative analysis, first, a maximum displacement, D_d , is assumed for the FPB. The assumed displacement, the bearing reactions due to the self-weight of the bridge, the friction coefficient (4%) and the radius, R (1020 mm), of the bearings are substituted in Eq. 3 to calculate the ELS for each bearing. The calculated ELS is then used to obtain the stiffness of the beam elements used in the model. The EVDR is also calculated by substituting the bearing properties and the assumed displacement in Eq. 4 to incorporate the effect of hysteretic energy dissipated by the isolation bearings in the analyses using a design response spectrum with damping equal to the calculated EVDR for the isolated modes of vibration. The MMRS analyses of the bridges are then conducted and new bearing displacements are obtained. The obtained displacements are compared with the initially assumed bearing displacements. If the difference is smaller than an assumed level of accuracy, the iteration is stopped; otherwise, the iteration is continued with the new displacements until the desired convergence is achieved.

ANALYSES RESULTS FOR BRIDGE-I

Periods of Vibration and Percentages of Modal Mass Participation

Table 2 presents the periods of vibration and percentages of modal mass participation for Bridge-I for the first five vibration modes including and excluding SSI effects for AASHTO soil types II, III-a and III-b. For all the soil types, the first two vibration modes, which are the fundamental vibration modes of the bridge in the transverse and longitudinal directions, are directly associated with the movement of the isolation system. The rest of the vibration modes involve the vibration of the substructures. The results presented in Table 2 reveal that including the SSI in the seismic analysis of the bridge for both the stiff and soft soil conditions does not affect the fundamental vibration periods of the bridge significantly. This results from (i) very small lateral stiffness of the isolation system relative to that of the substructures, (ii) larger mass of the superstructure and (iii) smaller mass of the substructure as observed from Eq. 1. However, it is found that including the SSI in the seismic analysis of the bridge significantly affects the periods at higher modes of vibration, which are related to the vibration of the substructures For the case involving SSI, further reduction of the foundation soil stiffness does not influence the periods

significantly at higher modes of vibration as observed from the analyses results for AASHTO soil type III-a and III-b,

Table 2 Bridge-I modal periods of vibration and percentage of modal mass participation

AASHTO Soil Type	Mode #	SSI Included			SSI Excluded		
		Period (s)	Percentage of Mass Participation		Period (s)	Percentage of Mass Participation	
			Long.	Trans.		Long.	Trans.
II	1	1.55	56.8	0.0	1.54	74.7	0.0
	2	1.52	0.0	56.2	1.51	0.0	74.0
	3	0.51	0.0	0.0	0.21	0.0	0.0
	4	0.24	10.1	0.0	0.15	0.0	0.0
	5	0.23	0.0	10.5	0.15	0.0	0.0
III-a	1	1.67	56.7	0.0	1.66	74.6	0.0
	2	1.65	0.0	56.2	1.64	0.0	74.0
	3	0.53	0.0	0.0	0.21	0.0	0.0
	4	0.28	10.1	0.0	0.15	0.0	0.0
	5	0.25	0.0	11.3	0.15	0.0	0.0
III-b	1	1.68	56.8	0.0	1.66	74.6	0.0
	2	1.65	0.0	56.3	1.64	0.0	74.0
	3	0.54	0.0	0.0	0.21	0.0	0.0
	4	0.31	10.0	0.0	0.15	0.0	0.0
	5	0.26	0.0	13.2	0.15	0.0	0.0

Furthermore, for the case involving SSI, the percentage of mass participation at higher modes is much more significant compared to the case excluding SSI. This is due to the movement of the foundation system for the case involving SSI that leads to larger contribution of the substructure mass to the dynamic response of the bridge. Nevertheless, as the mass of the substructures is not large in such bridges, the contribution of the higher modes of vibration to the seismic response is not significant and may be neglected in the seismic analysis.

It is noteworthy that in the long period range, the amplitude of the response spectrum for AASHTO soil type III is larger than that of the response spectrum for AASHTO soil type II. Therefore, larger isolation bearing displacements are obtained for the case involving AASHTO soil type III. This resulted in smaller ELS (k_i), for the isolation bearings (see Eq. 3) and larger fundamental period (see Eq. 1). Accordingly, the difference between the fundamental vibration periods of the bridge for AASHTO soil types II and III is due to the disparity in the amplitude of the spectra used in the analyses rather than the stiffness of the foundation soil.

Isolation Bearing Forces and Relative Displacements

Table 3 displays the isolation bearing seismic lateral forces and displacements for Bridge-I including and excluding SSI effects for different AASHTO soil types. These results reveal that including the SSI in the seismic analysis of the bridge for all the soil types has only a negligible effect on bearing seismic forces and displacements. It is noteworthy that the isolation bearing seismic lateral forces and relative displacements for the case involving AASHTO soil types III-a and III-b are larger than those of the case involving AASHTO soil type II. This is again due to the disparity in the amplitude of the spectra used in the analyses rather than the stiffness of the foundation soil. However, this clearly indicates that, in soft soil conditions the seismic force and displacement demands on the isolation bearings may be quite large.

Table 3 Bridge-I isolator seismic lateral forces and relative displacements

AASHTO Soil Type	Substr.	SSI Included				SSI Excluded			
		Long.		Trans.		Long.		Trans.	
		Lat. Force (kN)	Rel. Disp. (mm)						
II	N. Abut.	6.4	53	6.2	50	6.6	54	6.4	53
	Pier 1	27.9	51	27.9	51	28.2	52	28.5	53
	Pier 2	26.4	51	26.4	51	26.7	52	27.0	53
III-a	S. Abut.	4.8	53	4.7	50	5.0	54	4.8	53
	N. Abut.	8.2	79	7.8	74	8.3	81	8.3	80
	Pier 1	35.2	75	35.8	77	35.8	77	36.4	79
III-b	Pier 2	33.3	75	33.9	77	33.9	77	34.4	79
	S. Abut.	6.1	79	5.9	74	6.2	81	6.2	80
	N. Abut.	8.3	81	7.9	75	8.3	81	8.3	80
	Pier 1	35.8	77	36.1	78	35.8	77	36.4	79
	Pier 2	33.9	77	34.2	78	33.9	77	34.4	79
	S. Abut.	6.2	81	6.0	75	6.2	81	6.2	80

Seismic Forces at Pier Bases

Table 4 presents the reactions at the base of Bridge-I piers including and excluding SSI effects for various AASHTO soil types. The pier base shear forces for the case including SSI are slightly larger than those of the case excluding SSI. In the structural model without the SSI, the abutments are modeled as rigid supports. Therefore, relatively larger shear forces are transferred to the abutments and smaller shear forces are transferred to the piers compared to the case with SSI. The same trend is also observed for the pier base moment. However, the pier base moment becomes smaller than that of the case excluding SSI as the foundation soil becomes softer. This is mainly due to the smaller rotational stiffness of the pier base that leads to smaller moment.

Furthermore, for the analyses results involving SSI, the larger seismic forces at the base of the piers for softer foundation soil conditions can once more be explained by the disparity between the amplitudes of the response spectra for stiff and soft soil conditions. Nevertheless, the results presented in Table 4 reveal that for seismic-isolated bridges with heavy superstructures and light substructures, including SSI effects in the seismic analysis for stiff soil conditions may have only a negligible effect on the substructure reactions. However, SSI effects need to be included in the seismic analyses for soft soil conditions.

Table 4 Bridge-I support reactions at pier bases

AASHTO Soil Type	Pier	SSI Included				SSI Excluded			
		Long.		Trans.		Long.		Trans.	
		V (kN)	M (kN.m)	V (kN)	M (kN.m)	V (kN)	M (kN.m)	V (kN)	M (kN.m)
II	1	243	1110	259	1292	220	1020	233	1330
	2	227	941	225	1170	209	929	221	1212
III-a	1	278	1280	281	1542	260	1284	256	1598
	2	263	1162	287	1530	249	1175	246	1551
III-b	1	277	1277	257	1436	260	1284	256	1598
	2	262	1159	247	1379	249	1175	246	1551

ANALYSES RESULTS FOR BRIDGE-II

Periods of Vibration and Percentages of Modal Mass Participation

Table 5 presents the periods of vibration and percentages of modal mass participation for Bridge-II for the first five vibration modes including and excluding SSI effects for various AASHTO soil types. For all the soil types, the first vibration mode is directly associated with the relative movement of the isolation system in the transverse direction of the bridge. The rest of the vibration modes involve the vibration of the substructures. The results presented in Table 5 reveal that the effect of the SSI on the fundamental vibration periods of seismic isolated bridges with light superstructures and heavy substructures is not considerable for stiff soil conditions, but becomes more significant in the case of softer soil conditions. As observed from Eq. 1, this results from (i) the large mass of the substructures, (ii) the flexibility of the pile-soil system at the pier foundations, as well as (iii) the relatively smaller mass of the superstructure. However, at higher modes of vibration, which are related to the vibration of the substructures, the ratio of the vibration periods including and excluding SSI is found to be as much as 10.7. This may significantly affect the seismic response of the bridge due to the very large mass of the substructures. Therefore, higher modes of vibration need to be included in the seismic analysis.

Table 5 Bridge-II modal periods of vibration and percentage of modal mass participation

AASHTO Soil Type	Mode #	SSI Included			SSI Excluded		
		Period (s)	Percentage of Mass Participation		Period (s)	Percentage of Mass Participation	
			Long.	Trans.		Long.	Trans.
II	1	1.45	0.00	47.35	1.44	0.00	41.25
	2	0.57	77.14	0.00	0.29	0.00	0.00
	3	0.57	0.00	0.00	0.13	68.32	0.00
	4	0.54	0.02	0.00	0.09	0.00	0.00
	5	0.47	0.00	46.02	0.07	0.10	0.00
III-a	1	1.64	0.00	51.51	1.55	0.00	41.25
	2	0.70	11.95	0.00	0.29	0.00	0.00
	3	0.66	70.40	0.12	0.13	68.78	0.00
	4	0.64	0.16	41.94	0.09	0.01	0.00
	5	0.63	3.93	0.03	0.07	0.00	0.00
III-b	1	1.82	0.02	60.31	1.55	0.00	41.25
	2	0.90	16.80	0.19	0.29	0.00	0.00
	3	0.87	38.86	5.04	0.13	68.78	0.00
	4	0.85	9.81	28.08	0.09	0.01	0.00
	5	0.75	11.79	0.06	0.07	0.00	0.00

Isolation Bearing Forces and Relative Displacements

Table 6 displays the isolation bearing seismic lateral forces and displacements for Bridge-II including and excluding SSI effects for various AASHTO soil types. These results reveal that including the SSI in the seismic analysis of the bridge for all the soil types has a notable effect on bearing seismic forces and especially displacements. This effect is more pronounced for softer foundation soil conditions. This is mainly due to the lateral movement and rocking motion of the substructures over the more flexible foundation system producing larger relative displacements at the isolation bearings' level. This clearly indicates that, in soft soil conditions, the seismic force and displacement demands on the isolation bearings may be quite large.

For the case where the SSI effects are neglected, the abutments are excluded from the structural model using fixed support conditions at the abutment locations. Accordingly, the two abutments equally resist

the longitudinal seismic force. However, for the case where SSI effects are included in the analysis, only the abutment being pushed towards the backfill can effectively resist the longitudinal seismic force. This resulted in a larger longitudinal direction seismic force in each abutment bearing compared to the case without SSI effects. The large difference between the fixed bearing forces proves the importance of including SSI effects in the analysis.

As the foundation soil becomes softer, the magnitude of the seismic force required to displace the abutments in the longitudinal direction becomes smaller. This results in smaller seismic forces in the abutment bearings as observed from Table 6 for AASHTO soil types III-a and III-b. Note that the slight increase in the magnitude of the longitudinal seismic force in the abutment bearings for AASHTO soil type III-a compared to that for AASHTO soil type II is again due to the disparity in the amplitude of the spectra for stiff and soft soil conditions.

Table 6 Bridge-II isolator seismic lateral forces and relative displacements

AASHTO Soil Type	Substr.	SSI Included				SSI Excluded			
		Long.		Trans.		Long.		Trans.	
		Lat. Force (kN)	Rel. Disp. (mm)						
II	E. Abut.	80.4	N/A	7.2	42	58.0	NA	7.1	41
	Pier 1	15.0	13	19.7	33	11.1	0.74	21.7	41
	Pier 2	15.0	13	19.7	33	11.1	0.74	21.7	41
III-a	W. Abut.	80.4	N/A	7.2	42	58.0	NA	7.1	41
	E. Abut.	83.8	N/A	9.8	72	58.3	N/A	8.7	59
	Pier 1	16.4	21	25.2	54	10.9	0.07	26.6	59
III-b	Pier 2	16.4	21	25.2	54	10.9	0.07	26.6	59
	W. Abut.	83.8	N/A	9.8	72	58.3	NA	8.7	59
	E. Abut.	56.9	N/A	13.0	107	58.3	N/A	8.7	59
	Pier 1	23.1	46	31.6	78	10.9	0.07	26.6	59
	Pier 2	23.1	46	31.6	78	10.9	0.07	26.6	59
	W. Abut.	56.9	N/A	13.0	107	58.3	NA	8.7	59

Seismic Forces at Pier Bases

Table 7 presents the seismic reactions at the base of Bridge-II piers including and excluding SSI effects for various AASHTO soil types. The seismic shear forces at the pier base for the case including SSI effects are generally larger than those of the case excluding SSI. In the structural model without the SSI, the abutments are modeled as rigid supports. Therefore, relatively larger seismic shear forces are transferred to the abutments and smaller seismic shear forces are transferred to the piers than those of the cases with SSI effects. Additionally, in the case of the structural model with SSI effects, the seismic inertial forces generated by the product of the mass of the pier footing and acceleration at the flexible pier bases are automatically incorporated in the seismic response. Such inertial forces are not incorporated in the case of the model without SSI as the bases of the piers are modeled as fixed supports. Moreover, the contribution of the mass of the pier walls to the seismic response is more pronounced in the case of the model with SSI effects due to the larger seismic accelerations associated with the movement of the flexible foundation system. All these effects result in larger seismic shear forces at the base of the piers for the case including SSI. However, the seismic shear forces at the pier bases tend to become smaller as the foundation soil stiffness decreases. This results from larger vibration periods of the bridge for softer foundation soil conditions that produce smaller spectral accelerations, hence smaller inertial forces due to the shape of the acceleration spectrum.

In the longitudinal direction, the seismic moments at the pier base for the case including SSI effects for AASHTO Soil types II and III-a are slightly larger than those of the case excluding SSI. This is mainly due to the larger seismic shear forces generated at the pier bases. Furthermore, as the pier walls are relatively flexible in the longitudinal direction, the rotational flexibility of the foundation system does not influence the seismic base moments as much as expected. However, this is not true for softer foundation soil conditions where the seismic moments at the pier base for the case including SSI are larger than those of the case excluding SSI. In this case, the rotational flexibility of the foundation system becomes very small yielding smaller moments at the pier base.

In the transverse direction, the seismic moments at the base of the piers for the case including SSI effects are much smaller than those of the case excluding SSI. The difference is as much as 42%. For the case without the SSI, the very large stiffness of the fixed-base pier wall results in relatively larger seismic base moments compared to the case with SSI where rotation at the pier base is allowed to some extent due to the rotational flexibility of the foundation system. However, for softer foundation soil conditions, the seismic moments at the pier bases tend to increase as observed from the results presented in Table 7. This is mainly due to the excessive rocking of the pier walls producing larger moments at the base of the piers. The results presented in Table 7 reveal that for seismic-isolated bridges with light superstructures and heavy substructures, including SSI effects in the seismic analysis for both soil types may have a considerable effect on the substructure reactions.

Table 7 Bridge-II support reactions at pier bases

AASHTO Soil Type	Pier	SSI Included				SSI Excluded			
		Long.		Trans.		Long.		Trans.	
		V (kN)	M (kN.m)	V (kN)	M (kN.m)	V (kN)	M (kN.m)	V (kN)	M (kN.m)
II	1	321	1560	440	2040	203	1345	338	2900
	2	321	1560	440	2040	203	1345	338	2900
III-a	1	338	1538	482	2342	211	1420	369	3252
	2	338	1538	482	2342	211	1420	369	3252
III-b	1	201	911	425	2581	211	1420	369	3252
	2	201	911	425	2581	211	1420	369	3252

CONCLUSIONS

The effect of SSI on the seismic performance of seismic-isolated bridges is studied using two typical bridges with distinct features representing those bridges with (i) heavy superstructure and light substructure and (ii) light superstructure and heavy substructure. The conclusions are summarized as follows:

The effect of SSI on the fundamental vibration periods of seismic isolated bridges with heavy superstructure and light substructures is found to be negligible. However, it is observed that SSI may significantly affect the periods at higher modes of vibration, which are related to the vibration of the substructures. Nevertheless, as the mass of the substructures is not large in such bridges, the contribution of the higher modes of vibration to the seismic response is not significant and may be neglected in the analysis.

For seismic isolated bridges with heavy superstructure and light substructure, it is found that including the SSI in the seismic analysis of the bridge has only a negligible effect on isolation bearings' seismic forces and displacements regardless of the stiffness of the foundation soil. Similarly, including SSI in

the seismic analysis of such bridges is found to have a negligible effect on the substructure reactions for stiff soil conditions. However, including SSI in the seismic analysis is found to affect the magnitude of the substructure reactions for soft soil conditions.

The effect of SSI on the fundamental vibration period of seismic isolated bridges with light superstructures and heavy substructures is not considerable for stiff soil conditions but becomes more significant in the case of softer soil conditions. However, it is found that at higher modes of vibration, which are related to the vibration of the substructures, the ratio of the vibration periods including and excluding SSI may be as much as 10.7. This may significantly affect the seismic response of the bridge at higher modes of vibration due to the very large mass of the substructures. Therefore, higher modes of vibration need to be included in the analysis.

For seismic isolated bridges with light superstructures and heavy substructures, including the SSI in the seismic analysis is found to have a notable effect on bearing seismic forces and especially displacements. This effect is more pronounced for softer foundation soil conditions. Moreover, for such bridges, including SSI in the seismic analysis is observed to have a remarkable effect on the substructure reactions regardless of the foundation soil stiffness.

In summary, SSI may be neglected for seismic isolated bridges with heavy superstructure and light substructure constructed on stiff soil. However, SSI needs to be considered for bridges with light superstructure and heavy substructures regardless of the stiffness of the foundation soil. In soft soil conditions, SSI need to be considered regardless of the bridge type.

REFERENCES

1. Chaudhary, M T. A., Abe, M. and Fujino, Y. (2001), "Identification of soil-structure interaction effect in base-isolated bridges from earthquake", *Soil Dynamics and Earthquake Engineering*, 21 (8), 713-7252.
2. Vlassis, A. G. and Spyarakos, C.C. (2001), "Seismically isolated bridge piers on shallow soil stratum with soil-structure interaction", *Computers and Structures*, 79 (32), 2847-2861.1.
3. Todorovska, M. I., (1996), "Soil-structure interaction for base-isolated buildings", *Proceedings of 11th Conference on Engineering Mechanics*, ASCE, Volume 1, 172-175.
4. Dasgupta, S., Dutta, S. C and Bhattacharya, G. (1999) "Effect of soil-structure interaction on building frames on isolated footings" *Journal of Structural Engineering (Madras)*, 26 (2), 129-134
5. Dicleli, M. and Mansour, M. Y., (2002) "Seismic Retrofitting of Highway Bridges Using Friction Pendulum Seismic Isolation Bearings", Technical Report: BU-CEC-02-01, Department of Civil Engineering and Construction, Bradley University, Peoria IL.
6. AASHTO, (1998) LRFD Bridge Design Specifications, Washington, D.C, 1998.
7. AASHTO, (1999) Guide Specifications for Seismic Isolation Design, Washington, D.C.,.
8. SAP2000, (1998) Integrated Finite Element Analysis and Design of Structures, Computers and Structures Inc., Berkeley, California.
9. Novak, M., (1977) "Vertical vibration of floating piles", *ASCE Journal of Engineering Mechanics*, 103 (EMI), 153-168.
10. Dobry, R. and Gazetas, G., (1986) "Dynamic Response of Arbitrary Shaped Foundations", *ASCE Journal of Geotechnical and Geoenvironmental Engineering*, 112(2), 109-135.
11. FHWA, (1997) Geotechnical Engineering Circular No 3 – Design Guidance: Geotechnical Earthquake Engineering for Highways – Volume I - Design Principles, Publication No. FHWA-SA-97-076 Federal Highway Administration, US Department of Transportation, Washington, D.C..
12. Clough, G. W. and Duncan, J. M., (1991) *Foundation Engineering Handbook*, 2nd Edition, Edited by H. Y. Fang, Van Nostrand Reinhold, New York, NY, 223-235.

